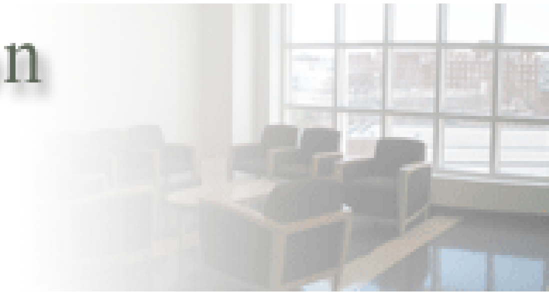

Detection, Reconstruction and Approximate Evolution of Piecewise Smooth Solutions

Eitan Tadmor

Center for Scientific Computation and Mathematical Modeling (CSCAMM)
Department of Mathematics, Institute for Physical Science & Technology
University of Maryland
www.cscamm.umd.edu/~tadmor

OUTLINE

- Piecewise smoothness
- A sense of direction

⊙ Direction of propagation vs. direction of smoothness

- Local methods — central schemes
  - ⊙ Detection of edges
  - ⊙ Reconstruction in direction of smoothness
- Global methods — spectral projections
  - ⊙ Detection of edges revisited
  - ⊙ Adaptive mollifiers

Regularity Spaces – Theory

- Propagation of waves: $\mathcal{E}(t): \ u_0(x) \in X_0 \longmapsto u(x,t) \in X(t)$

- Linear Transport: $u_t + a u_x = 0$

$$u(x,t) = u_0(x - at), \qquad \mathcal{E}(t): H^s \longmapsto H^s, \quad X = H^s$$

- Nonlinear Transport: $u_t + a(u) u_x = 0$

$\{u = u(x,t) | u = u_0(x - a(u)t)\}$, $\quad \mathcal{E}(t): L^\infty \longmapsto L^\infty$, $X = L^\infty$ too large...

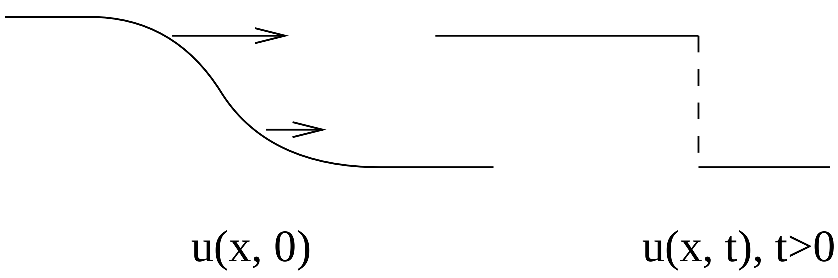

$$u_x(x,t) = \frac{u_{0x}}{1 + t a'(u_0) u_{0x}} \downarrow -\infty$$

$\odot$ $\mathcal{E}(t): BV \longmapsto BV \quad X = BV$ still too large...

Approximate solutions $\mathsf{w}^h(x,t)$

⊙ Local and global basis functions

∘ Piecewise polynomials: $\mathsf{w}^h(\cdot,t) = \sum_j p_j(\cdot,t)1_{C_j}(\cdot), \quad h \sim |C_k|$

∘ Wavelets, particle methods, ... :

$$\mathsf{w}^h(\cdot,t) = \sum_{jk} \widehat{\mathsf{w}}_{jk}(t)\psi_{jk}(\cdot), \quad h \sim \frac{1}{\#\left\{\widehat{\mathsf{w}}_{jk} \neq 0\right\}}$$

∘ Spectral methods: $\mathsf{w}^h(\cdot,t) = \sum_{|j|\le N} \widehat{\mathsf{w}}_j(t)e^{ij\cdot x} \quad h \sim \frac{1}{N}$

Theory: $\|\mathsf{w}^h(\cdot,t) - u(\cdot,t)\|_{L^1} \le Const \cdot \sqrt{h}$

⊙ sharp for BV data: $Const \sim \|u_0\|_{BV}$

Computations: $\|\mathsf{w}^h(\cdot,t) - u(\cdot,t)\|_{L^1} \sim h \quad$ ... but never $\sqrt{h}$

Piecewise Regularity Spaces – Computations

⊙ Theory — BV excludes spurious oscillations

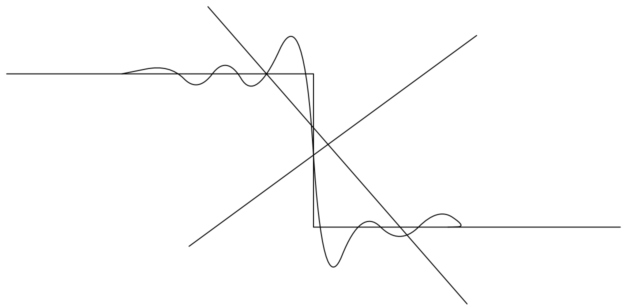

but may contain infinitely many jump discontinuities

⊙ Computations — can resolve only piecewise smooth data:

smooth data separated by finitely many jumps $- X_L(t) := \{x \mid u_x(x,t) \geq -L\}$

- (*ET.-Tang-Tassa*) $- \|u(x,t)\|_{C^s(X_L(t))} \leq e^{sLt}\|u_0\|_{C^s(X_L(0))}$

$$\|w^h(\cdot,t) - u(\cdot,t)\|_{L^1} = Const.h|\log(h)|$$

Nonlinear convection

- Conservation laws – integral balance statements:

$$\frac{\partial}{\partial t}u(x,t) + \nabla_x \cdot f(u(x,t)) = 0, \quad u := (u_1, \ldots, u_m)^\top$$

- Hamilton-Jacobi equations: $\frac{\partial}{\partial t}u(x,t) + H(t,x,u,\nabla_x u(x,t)) = 0$

- Eulerian dynamics: $\frac{\partial}{\partial t}u(x,t) + (u \cdot \nabla_x)u = F$

⊙ Formation of shocks, non-differentiable kinks, slip lines,...

- Theory: $X(t) = BV, BUC, \ldots$

⊙ Complete scalar BV theory – $m = 1$ (*Kruzkov*)

⊙ BV solutions for d=1-systems (*Lax,Glimm,Bressan..*)

⊙ Complete theory of viscosity solutions (*Crandall-Lions,...*)

⊙ Little is known for $(m-1) \times (d-1) > 0$ — (*Computations...*)

- Computations $X(t)$ = piecewise smoothness

Sense of Direction. I: Direction of propagation $u_t + f(u)_x = 0$

- *Godunov*: $\mathrm{w}^h(x,t) = \sum_j \overline{\mathrm{w}}_j(t) 1_{[x_{j-\frac{1}{2}}, x_{j+\frac{1}{2}}]}(x)$

$$div_{t,x}(u, f(u)) = 0$$

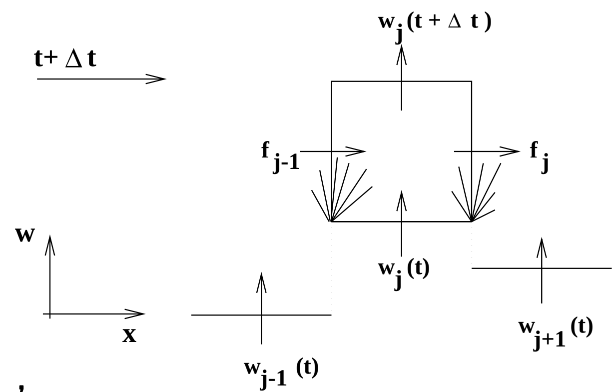

$$\boxed{\overline{\mathrm{w}}_j(t+\Delta t) = \overline{\mathrm{w}}_j(t) - \frac{\Delta t}{\Delta x}\left(f(\mathrm{w}_{j+\frac{1}{2}}(t)) - f(\mathrm{w}_{j-\frac{1}{2}}(t))\right)}$$

⊙ $\mathrm{w}_{j\pm\frac{1}{2}}$ are computed by Riemann solvers – ' upwinding'

- *Lax-Friedrichs* –

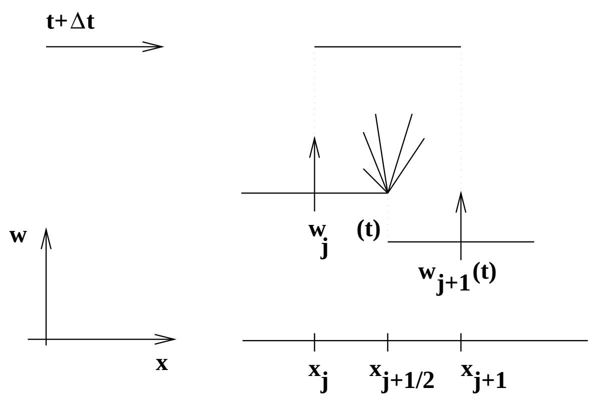

$$\boxed{\overline{\mathrm{w}}_{j+\frac{1}{2}}(t+\Delta t) = \frac{1}{2}(\overline{\mathrm{w}}_j(t) + \overline{\mathrm{w}}_{j+1}(t)) - \frac{\Delta t}{2\Delta x}(f(\overline{\mathrm{w}}_{j+1}(t)) - f(\overline{\mathrm{w}}_j(t)))}$$

⊙ central scheme - no Riemann solvers; more viscous

Sense of Direction. II Direction of smoothness

- Macro-scale features of non-smoothness –

> ...barriers for propagation of smoothness

- High-resolution – discrete stencils do not cross discontinuities

$$\overline{\mathrm{w}}_j(t + \Delta t) = \mathcal{F}(\overline{\mathrm{w}}_{j-p}(t), \ldots, \overline{\mathrm{w}}_{j+p}(t))$$

1. Detection of edges
2. Non-oscillatory reconstruction in direction of smoothness

$$\begin{aligned} \mathrm{w}^h(x) &= \mathcal{R}_h \sum_j \overline{\mathrm{w}}_j 1_{C_j}(x) \longmapsto \sum_j p_j(x) 1_{C_j}(x) \\ p_j(x) &= \mathrm{w}_j + \mathrm{w}'_j(x - x_j) + \frac{\mathrm{w}''_j}{2}(x - x_j)^2 + \ldots \end{aligned}$$

Reconstruction in direction of smoothness. 1D Local methods

⊙ Edge detections: $D_+\overline{\text{w}}_j := \frac{\overline{\text{w}}_{j+1}-\overline{\text{w}}_j}{\Delta x}, D_-\overline{\text{w}}_j := \frac{\overline{\text{w}}_j-\overline{\text{w}}_{j-1}}{\Delta x}$...

$$\begin{aligned}
\text{w}_j &= \overline{\text{w}}_j + \ldots \\
\text{w}'_j &:= mm(D_-\overline{\text{w}}_j, D_+\overline{\text{w}}_j) = \theta_j D_+\overline{\text{w}}_j \sim \text{w}_x \\
\text{w}''_j &:= \theta_j D_+ D_-\overline{\text{w}}_j \sim \text{w}_{xx}
\end{aligned}$$

⊙ $\theta_j =$ nonlinear limiter $\in [0, 1]$

⊙ Co-monotonicity (*van Leer, Roe, Harten, . . .*) – MUSCL, ENO

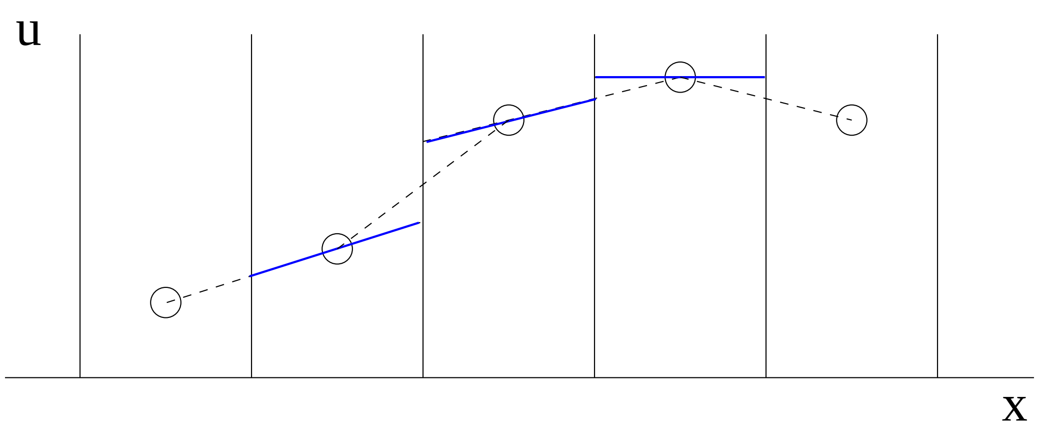

$$\| \sum_j [\overline{\text{w}}_j + \overline{\text{w}}'_j(x - x_j)] 1_{C_j}(x) \|_{BV} \leq \| \sum_j \overline{\text{w}}_j 1_{C_j}(x) \|_{BV}$$

- Library of non-linear, non-oscillatory numerical derivatives, $\{\text{w}\}'$, $\{\text{w}\}''$,...

2^{nd}-order central scheme (*Nessyahu-Tadmor*)

- Reconstruction $\mathcal{R}_{\Delta x}$

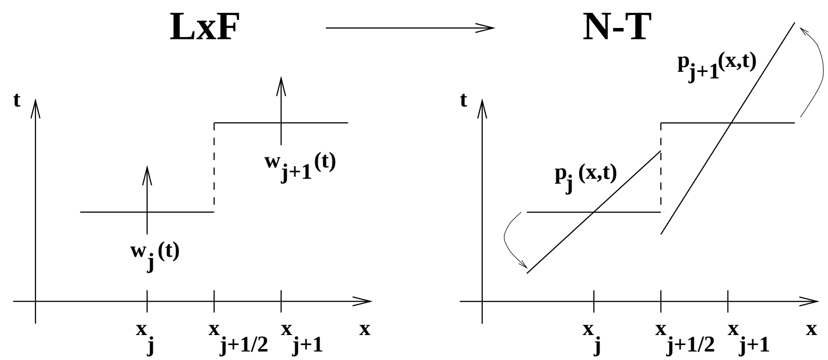

⊙ 2^{nd}-order non-oscillatory: $p_j(x,t^n) = \overline{\mathrm{w}}_j(t) + \mathrm{w}'_j(x-x_j)$, $\quad \mathrm{w}'_j \simeq \dfrac{\partial \mathrm{w}(x_j)}{\partial x}$

⊙ Numerical derivatives – component-wise. Example: $\mathrm{w}_j^{(k)\prime} = mm\left(D_+\mathrm{w}_j^{(k)}, D_-\mathrm{w}_j^{(k)}\right)$

- Evolution $\mathcal{E}(\Delta t)$ — Exact $\mathrm{w}(x,t^n) = \sum_j p_j(x,t^n) 1_{C_j}(x)$
- Projection $\mathcal{A}_{\Delta x}$ — solution is realized by cell averages

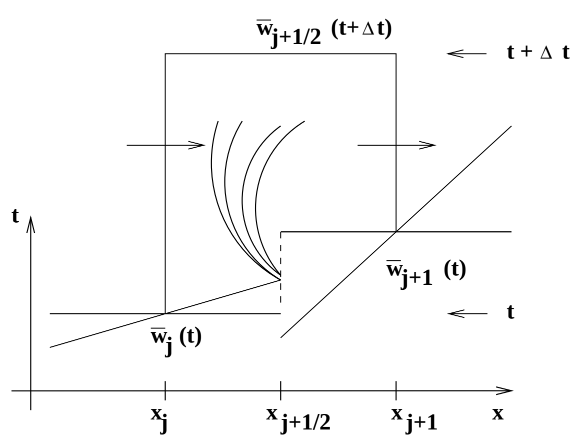

- Projection $P_{\Delta x} = \mathcal{R}_{\Delta x}\mathcal{A}_{\Delta x}$:

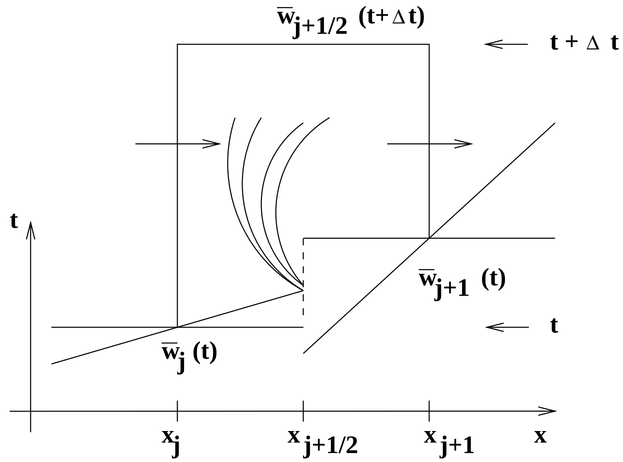

$$\overline{w}^{n+1}_{j+\frac{1}{2}} = \frac{1}{\Delta x}\left[\int_{x_j}^{x_{j+1/2}} p_j(x,t^n)dx + \int_{x_{j+1/2}}^{x_{j+1}} p_{j+1}(x,t^n)dx\right] - \frac{1}{\Delta x}\left[\int_{\tau=t^n}^{t^{n+1}} f(w_{j+1}(\tau))d\tau - \int_{\tau=t^n}^{t^{n+1}} f(w_j(\tau))d\tau\right]$$

Predictor – of mid-values

$$w_j^{n+\frac{1}{2}} = \overline{w}_j^n - \frac{\Delta t}{2} f'_j, \qquad f'_j = f_w(\overline{w}_j)\cdot \overline{w}'_j$$

Corrector: extracting information in direction of smoothness

$$\overline{w}^{n+1}_{j+\frac{1}{2}} = \frac{1}{2}(\overline{w}^n_j + \overline{w}^n_{j+1}) + \frac{\Delta x}{8}(w'_j - w'_{j+1}) - \frac{\Delta t}{\Delta x}\left[f(w^{n+\frac{1}{2}}_{j+1}) - f(w^{n+\frac{1}{2}}_j)\right]$$

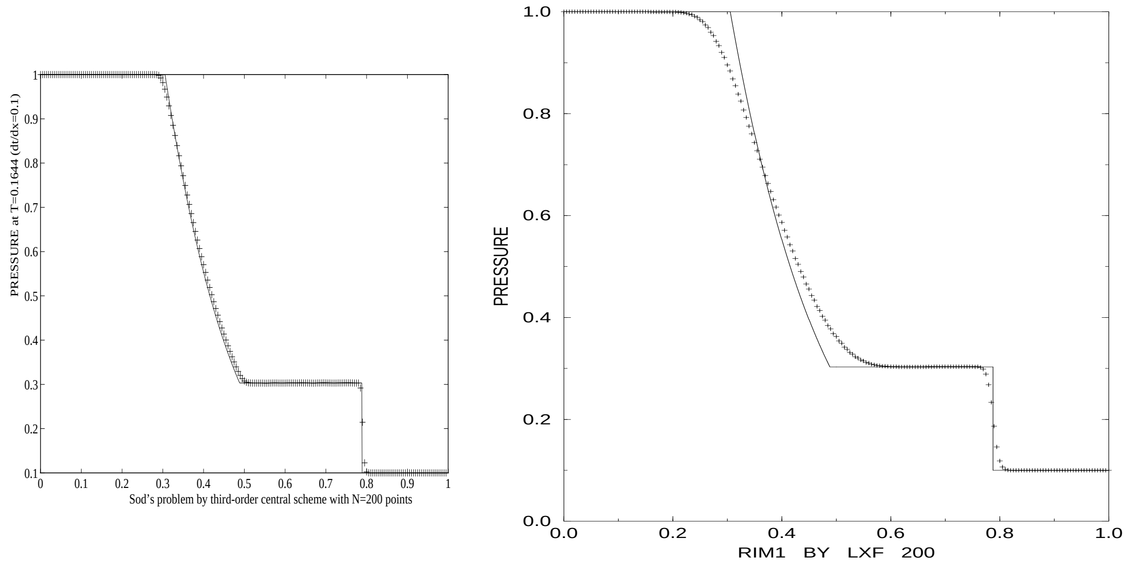

Sod's Riemann's problem solution by 2^{nd}-order central scheme, compared with 1^{st}-order Lax-Friedrichs scheme (*Nessyahu-Tadmor*).

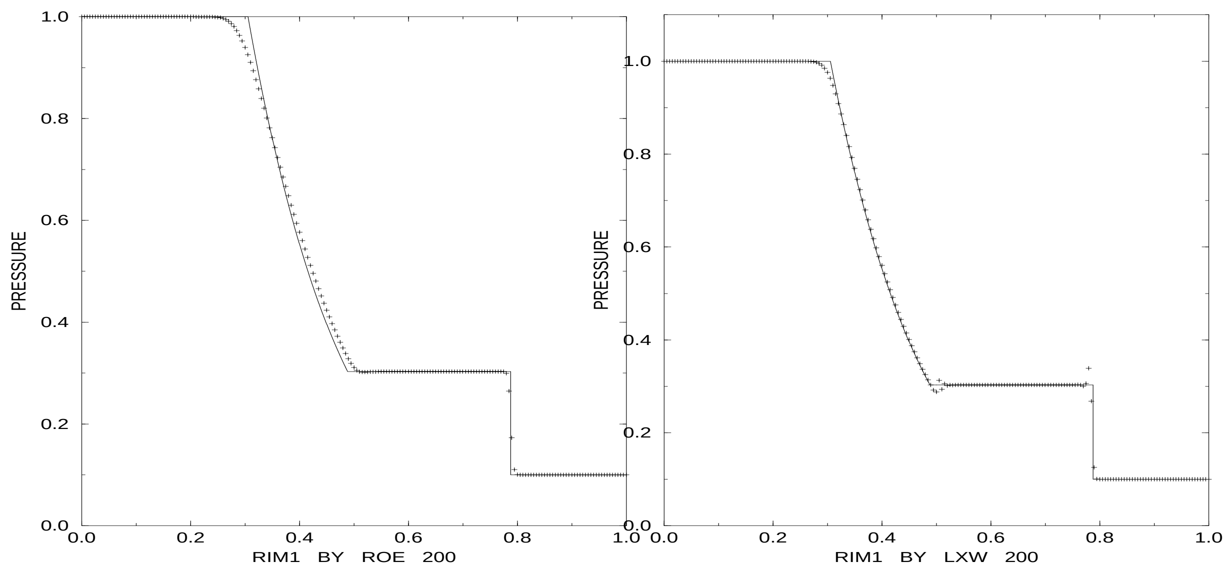

(**Left**) Sod's Riemann problem by 1^{st}-order Godunov – lack of resolution, and 2^{nd}-order Lax-Wendroff – spurious oscillations (**Right**).

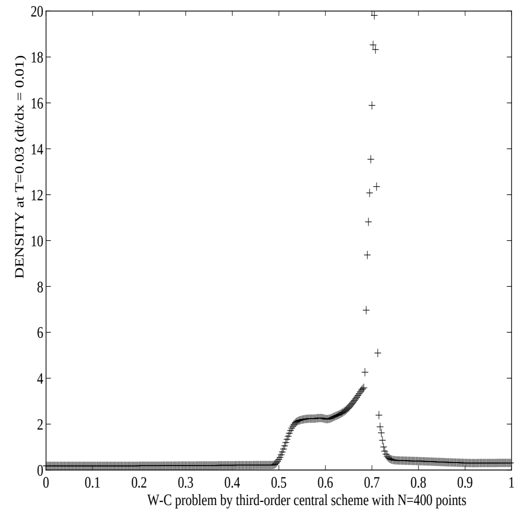

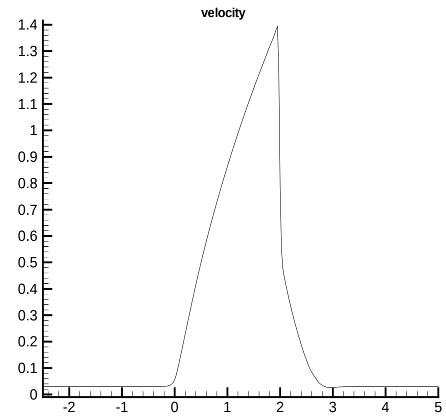

Left: 3^{rd}-order central simulation of Woodward-Colella banging problem with $N = 400$ cells (*Nessyahu-Tadmor*) . **Right**: 2^{nd}-order central scheme simulation of electron velocity in semiconductor device governed by 1D Euler-Poisson eq's; $N = 400$ cells (*Gardner-Gelb*).

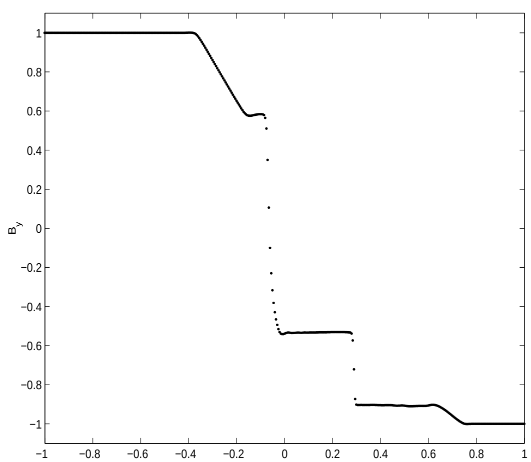

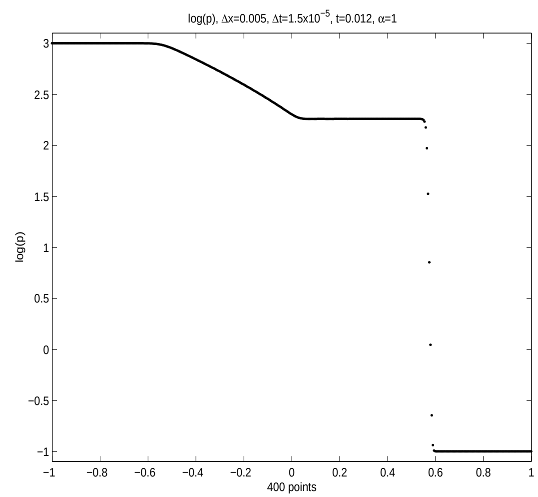

Left: 3^{rd}-order central scheme simulation of 1D MHD Riemann problem. with $N = 400$ cells; the y-magnetic field at $t = 0.2$, and **Right**: Pressure in high-Mach MHD Riemann problem (*Tadmor-Wu*).

Central schemes –extensions

- Multidimensional problems: $u_t + f(u)_x + g(u)_y = 0$

G.-S. Jiang-ET., P. Arminjon et. al., D. Kröner et. al.,...

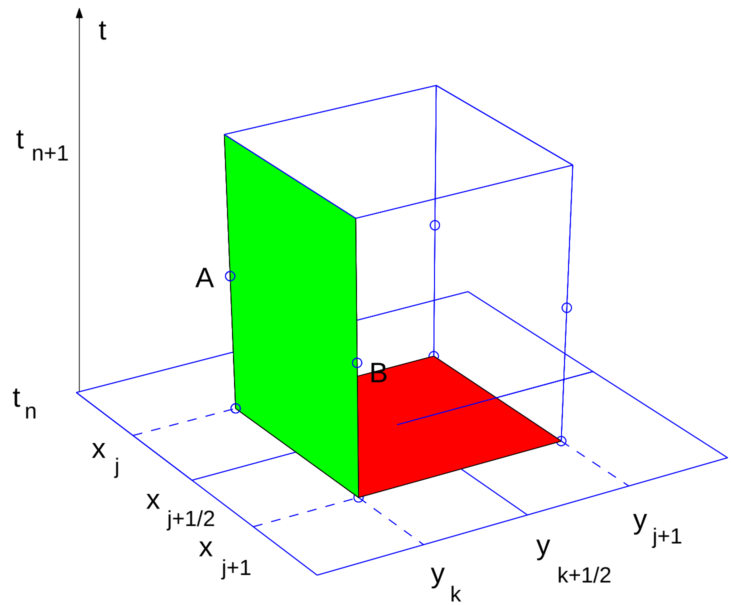

Reconstruction in direction of smoothness:

$$p_{j,k}(x,y) = \overline{\mathrm{w}}^n_{j,k} + \mathrm{w}'_{j,k}(x-x_j) + \mathrm{w}^{\backprime}_{j,k}(y-y_k) + \ldots,$$

$\odot$ $\mathrm{w}'_{j,k} = mm(D_{\pm x}\overline{\mathrm{w}}_{j,k}) \sim \mathrm{w}_x(x_j, y_k, t^n) + \mathcal{O}(\Delta x)^2$

$\odot$ $\mathrm{w}^{\backprime}_{j,k} = mm(D_{\pm y}\overline{\mathrm{w}}_{j,k}) \sim \mathrm{w}_y(x_j, y_k, t^n) + \mathcal{O}(\Delta y)^2$

$$\underline{\text{Evolution}} \quad \overline{w}^{n+1}_{j+\frac{1}{2},k+\frac{1}{2}} = \frac{1}{\Delta x \Delta y} \int\int_{C_{j+\frac{1}{2},k+\frac{1}{2}}} p(x,y,t^n)\,dy\,dx -$$

$$-\frac{1}{\Delta x \Delta y} \int_{\tau=t^n}^{t^{n+1}} \left\{ \int_{y=y_k}^{y_{k+1}} \left[f\left(w(x_{j+1},y,\tau)\right) - f\left(w(x_j,y,\tau)\right)\right] dy \right\} d\tau - \ldots$$

$$\underline{\text{Predictor}}: \quad \boxed{w^{n+\frac{1}{2}}_{j,k} = \overline{w}^n_{j,k} - \frac{\Delta t}{2} f'_{j,k} - \frac{\Delta t}{2} g^{\grave{}}_{j,k}}$$

$$\underline{\text{Corrector}}: \quad \left(< w_{j,\cdot} >_{k+\frac{1}{2}} := \tfrac{1}{2}(w_{j,k} + w_{j,k+1})\right)$$

$$\boxed{\begin{aligned} \overline{w}^{n+1}_{j+\frac{1}{2},k+\frac{1}{2}} \quad &= \quad < \frac{1}{4}(\overline{w}^n_{j,\cdot} + \overline{w}^n_{j+1,\cdot}) + \frac{\Delta x}{8}(w'_{j,\cdot} - w'_{j+1,\cdot}) - \frac{\Delta t}{\Delta x}(f^{n+\frac{1}{2}}_{j+1,\cdot} - f^{n+\frac{1}{2}}_{j,\cdot}) >_{k+\frac{1}{2}} + \\ &+ \quad < \frac{1}{4}(\overline{w}^n_{\cdot,k} + \overline{w}^n_{\cdot,k+1}) + \frac{\Delta y}{8}(w^{\grave{}}_{\cdot,k} - w^{\grave{}}_{\cdot,k+1}) - \frac{\Delta t}{\Delta y}(g^{n+\frac{1}{2}}_{\cdot,k+1} - g^{n+\frac{1}{2}}_{\cdot,k}) >_{j+\frac{1}{2}} \end{aligned}}$$

⊙ scalar maximum principle: $\mathcal{E}_h(t) : L^\infty \longmapsto L^\infty$

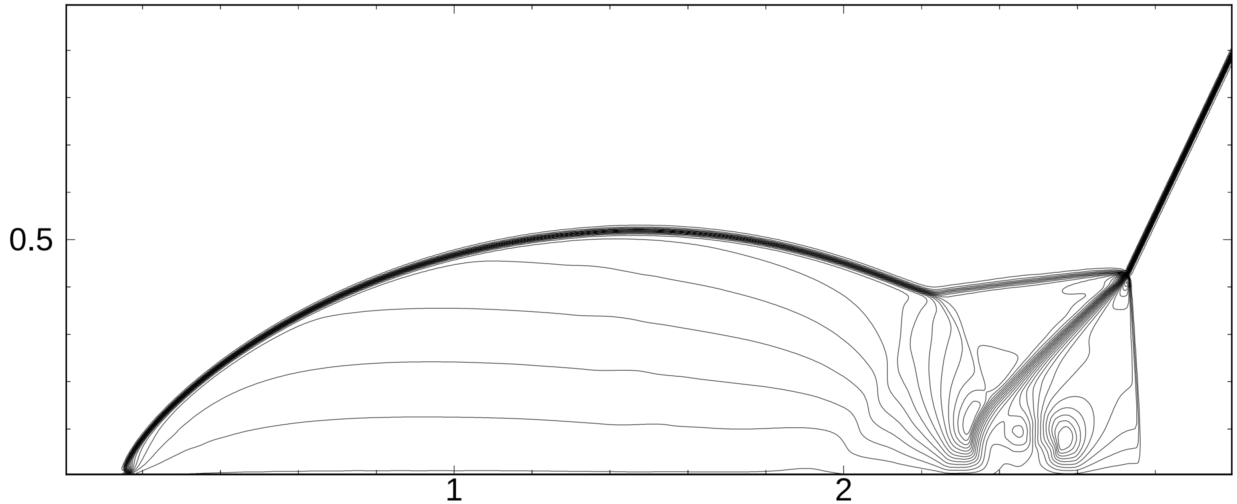

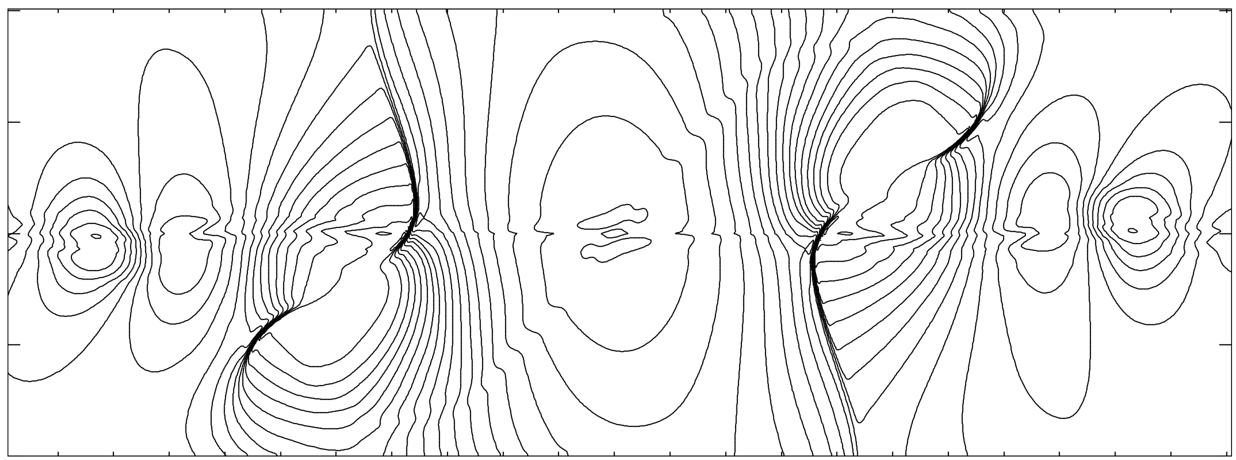

Top: Double Mach reflection problem. NT-MM1 960×240 grid points using JT-mm1 2^{nd}-order central scheme (*Jiang-Tadmor*).

Bottom: Pressure contours in Kelvin-Helmholtz instability $(B||v)$ using 2^{nd}-order central scheme (*Tadmor-Wu*).

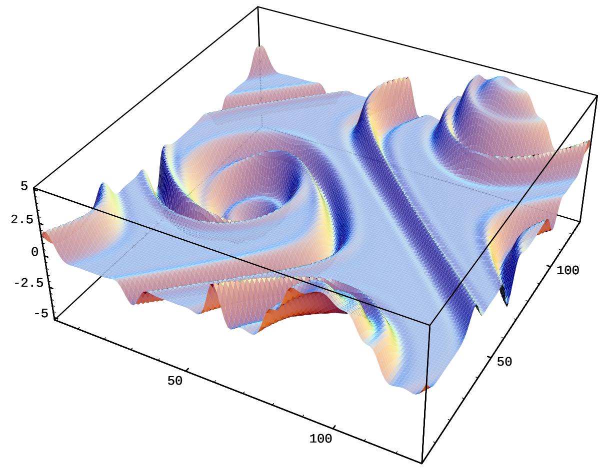

3^{rd}-order central scheme simulation of 'thick layer problem' $\omega_t + (u\omega)' + (v\omega)^\backprime = 0$ with 128^2 cells (*Levy-Tadmor*).

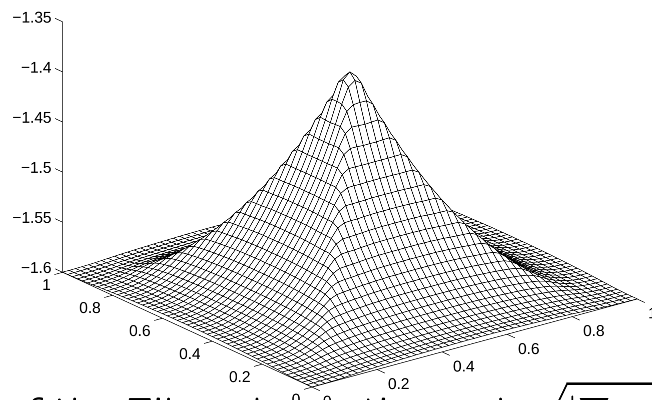

2^{nd}-order central simulation of the Eikonal equation $u_t + \sqrt{|\nabla_x u|^2 + 1} = 0$ with 50^2 gridvalues (*Lin-Tadmor*).

Central Schemes revisited Semi-discrete version
(*Kurganov-ET.*)

- Central schemes – dissipation of order $\mathcal{O}\left(\frac{(\Delta x)^{2r}}{\Delta t}\right)$
- Convection-diffusion eq's - dissipation $\mathcal{O}(\Delta x)^{2r-1}$

⊙ Local speeds: $a_{j\pm\frac{1}{2}}\Delta t$ replaces $\frac{\Delta x}{2}$

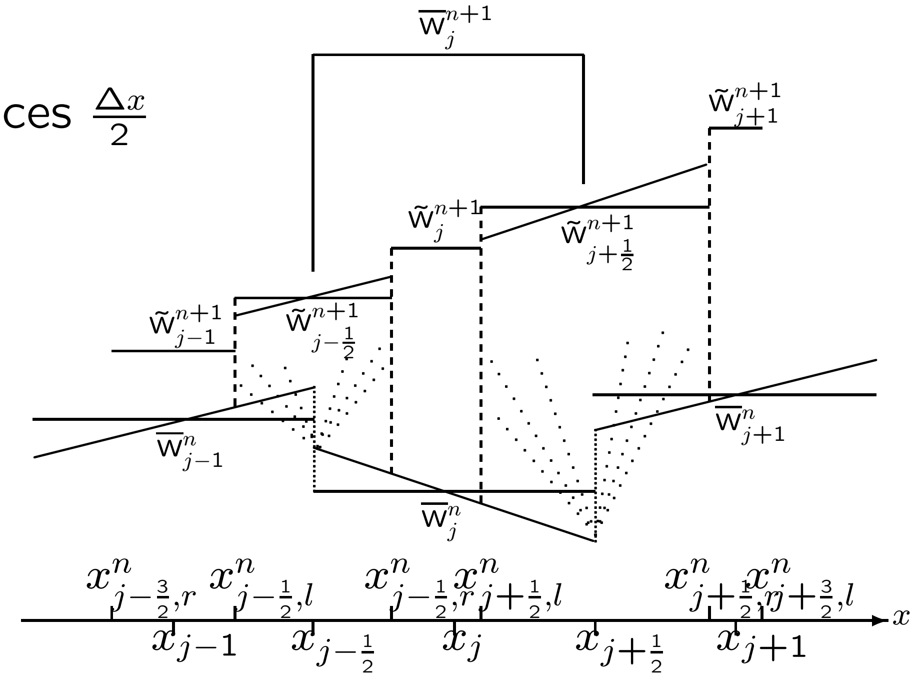

⊙ Reconstructed point-values ... in direction of smoothness ($w'_j(t)$)

$$w^{n+\frac{1}{2}}_{right} \longrightarrow \overline{w}_{j+1}(t)-\frac{\Delta x}{2}w'_{j+1}(t) \quad =: \quad w^{+}_{j+\frac{1}{2}}(t),$$

$$w^{n+\frac{1}{2}}_{left} \longrightarrow \overline{w}_{j}(t)+\frac{\Delta x}{2}w'_{j}(t) \quad =: \quad w^{-}_{j+\frac{1}{2}}(t),$$

⊙ $$\overline{w}^{n+1}_j = \overline{w}^n_j + \Delta t \cdot \mathcal{H}\left[w^{\pm}_{j\pm\frac{1}{2}}, f(w^{\pm}_{j\pm\frac{1}{2}}), a_{j\pm\frac{1}{2}}\right] + \mathcal{O}(\Delta t)^2$$

$$\frac{d}{dt}\overline{\mathrm{w}}_j(t) = -\frac{H_{j+\frac{1}{2}} - H_{j-\frac{1}{2}}}{\Delta x} \quad H_{j+\frac{1}{2}}(t) := \frac{f(\mathrm{w}^+_{j+\frac{1}{2}}) + f(\mathrm{w}^-_{j+\frac{1}{2}})}{2} - \frac{a_{j+\frac{1}{2}}}{2}\left[\mathrm{w}^+_{j+\frac{1}{2}} - \mathrm{w}^-_{j+\frac{1}{2}}\right]$$

⊙ $a_{j+\frac{1}{2}}(t)$ – max. local speed, $a_{j+\frac{1}{2}}(t) := \max_{\pm}\left\{\rho(\frac{\partial f}{\partial u}(\mathrm{w}^{\pm}_{j+\frac{1}{2}}))\right\}$

- 2D extension

$$\frac{d}{dt}\overline{\mathrm{w}}_{j,k}(t) = -\frac{H^x_{j+\frac{1}{2},k} - H^x_{j-\frac{1}{2},k}}{\Delta x} - \frac{H^y_{j,k+\frac{1}{2}} - H^y_{j,k-\frac{1}{2}}}{\Delta y}$$

$$H^x_{j+\frac{1}{2},k}(t) := \frac{f(\mathrm{w}^+_{j+\frac{1}{2},k}) + f(\mathrm{w}^-_{j+\frac{1}{2},k})}{2} - \frac{a^x_{j+\frac{1}{2},k}}{2}\left[\mathrm{w}^+_{j+\frac{1}{2},k} - \mathrm{w}^-_{j+\frac{1}{2},k}\right]$$

$$H^y_{j,k+\frac{1}{2}}(t) := \frac{g(\mathrm{w}^+_{j,k+\frac{1}{2}}) + g(\mathrm{w}^-_{j,k+\frac{1}{2}})}{2} - \frac{b^y_{j,k+\frac{1}{2}}}{2}\left[\mathrm{w}^+_{j,k+\frac{1}{2}} - \mathrm{w}^-_{j,k+\frac{1}{2}}\right]$$

⊙ Maximum principle: $\mathcal{E}_h(t) : L^\infty \longmapsto L^\infty$

- ODE solvers

⊙ 3rd and higher orders: *A. Kurganov, S.Noelle, G.Petrova,..*

- **Black Box** non-oscillatory solvers in direction of smoothness

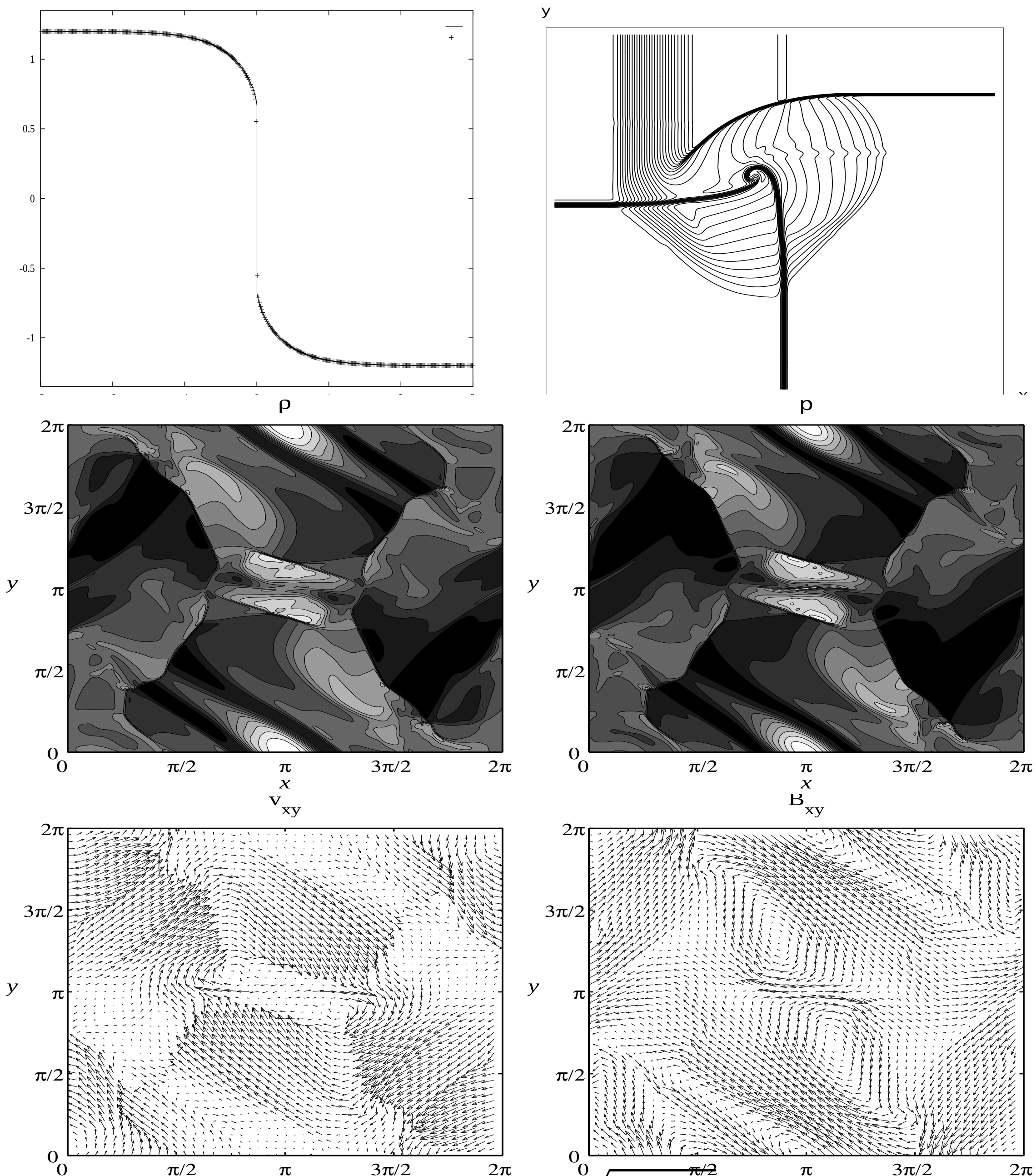

Top: (L) Saturating dissipation, $u_t + f(u)_x = (u_x/\sqrt{1+u_x^2})_x$ simulated by KT scheme with 400 cells (*Rosenau et. al.*). (R) 3^{rd}-order central scheme for 2D Riemann problem without Riemann solver. Density contours lines with 400×400 cells (*Kurganov-Tadmor*).

Bottom: Orszag-Tang problem by 2^{nd}-order central scheme with 384^2 cells (*Tadmor-Wu*).

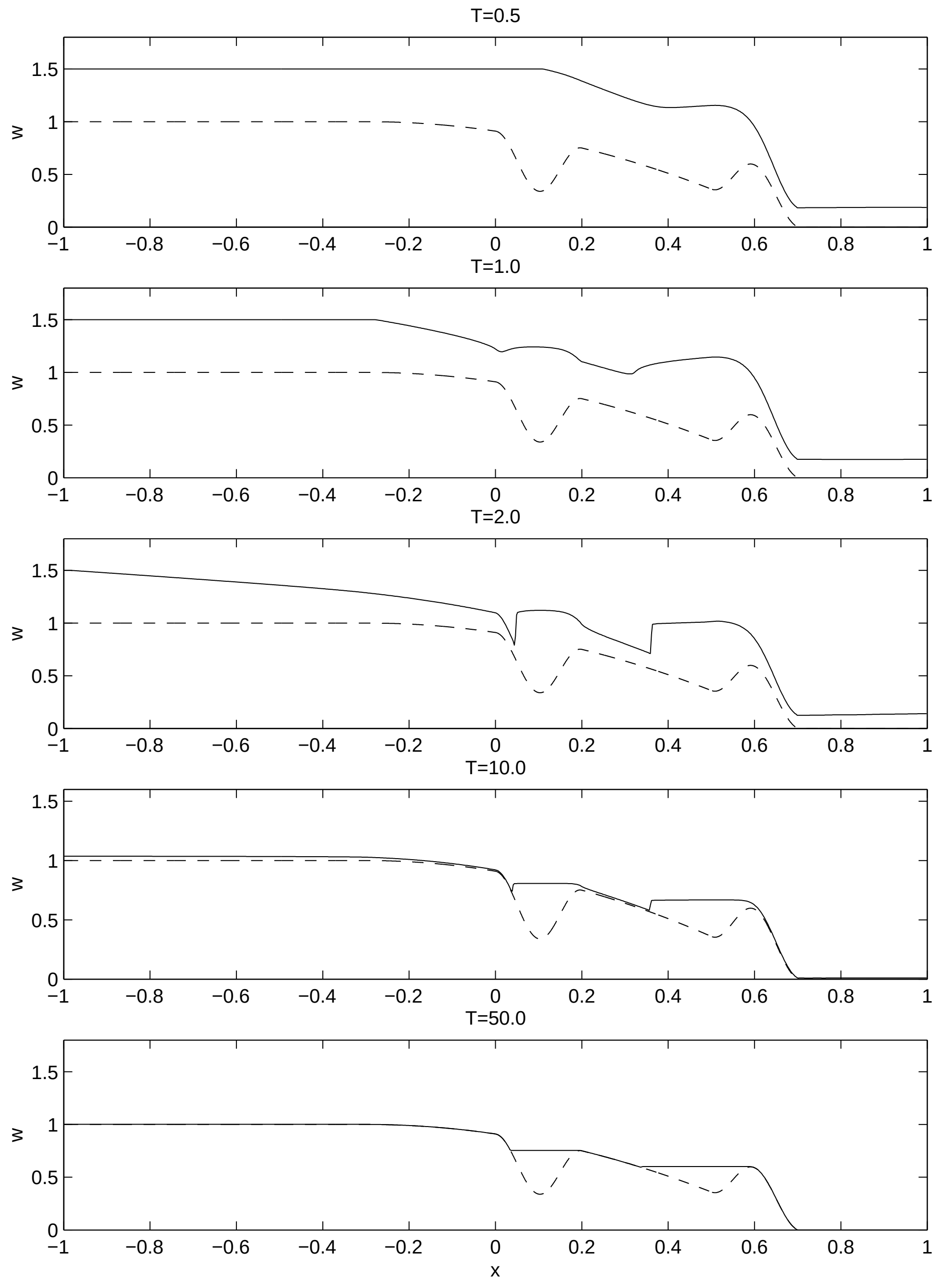

Steady flow of a river with given bottom topography. Solution of Saint-Venant system by 2^{nd}-order central scheme (*Kurganov-Levy*).

- Advantages of simplicity –

* Central schemes are free of (approximate) Riemann-solvers ...

* Do not require dimensional splitting ...

* Apply to arbitrary flux functions ...

- Provide effective high-resolution "black-box solvers":

Construction analysis & applications: *www.math.umd.edu/~tadmor/centralstation*

Multi-component problems	Relaxation problems
Extended thermodynamics	Semi-conductors
Incompressible flows	Shallow-water/Saint-Venant
Balance laws	Saturating dissipation
Homogenization	Discrete kinetic models
Hamilton-Jacobi eq's	MHD
The p-system	Injection
Riemann problems	Granular Avalanches
Flocculations, Fluctuations and related models	

- Key role: Data is realized as piecewise smooth

1. Detection of macro-scales of non-smoothness
2. Extracting information in direction of smoothness

Piecewise Regularity and High Resolution

Global Methods — small scale $h \sim \frac{1}{N}$

- We start with global moments: $\widehat{f}_k = \langle f, \phi_k \rangle$

$$S_N[f](x) = \sum_{-N}^{N} \widehat{f}_k e^{ikx}, \qquad \phi_k \longleftrightarrow e^{ikx}$$

⊙ Smooth f's: spectral/exponential accuracy ...

$$|S_N[f](x) - f(x)| \leq \begin{cases} \|f\|_{C^s} N^{-s} & \forall s \\ Const.e^{-\eta N} \end{cases}$$

⊙ Piecewise smooth f's: Gibbs' phenomenon

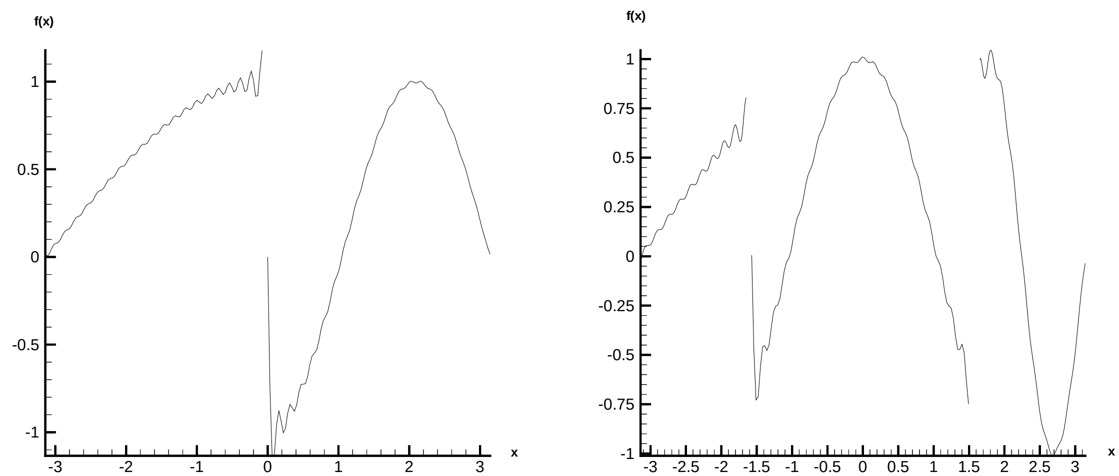

○ Spurious oscillations ('ringing'); first-order accuracy

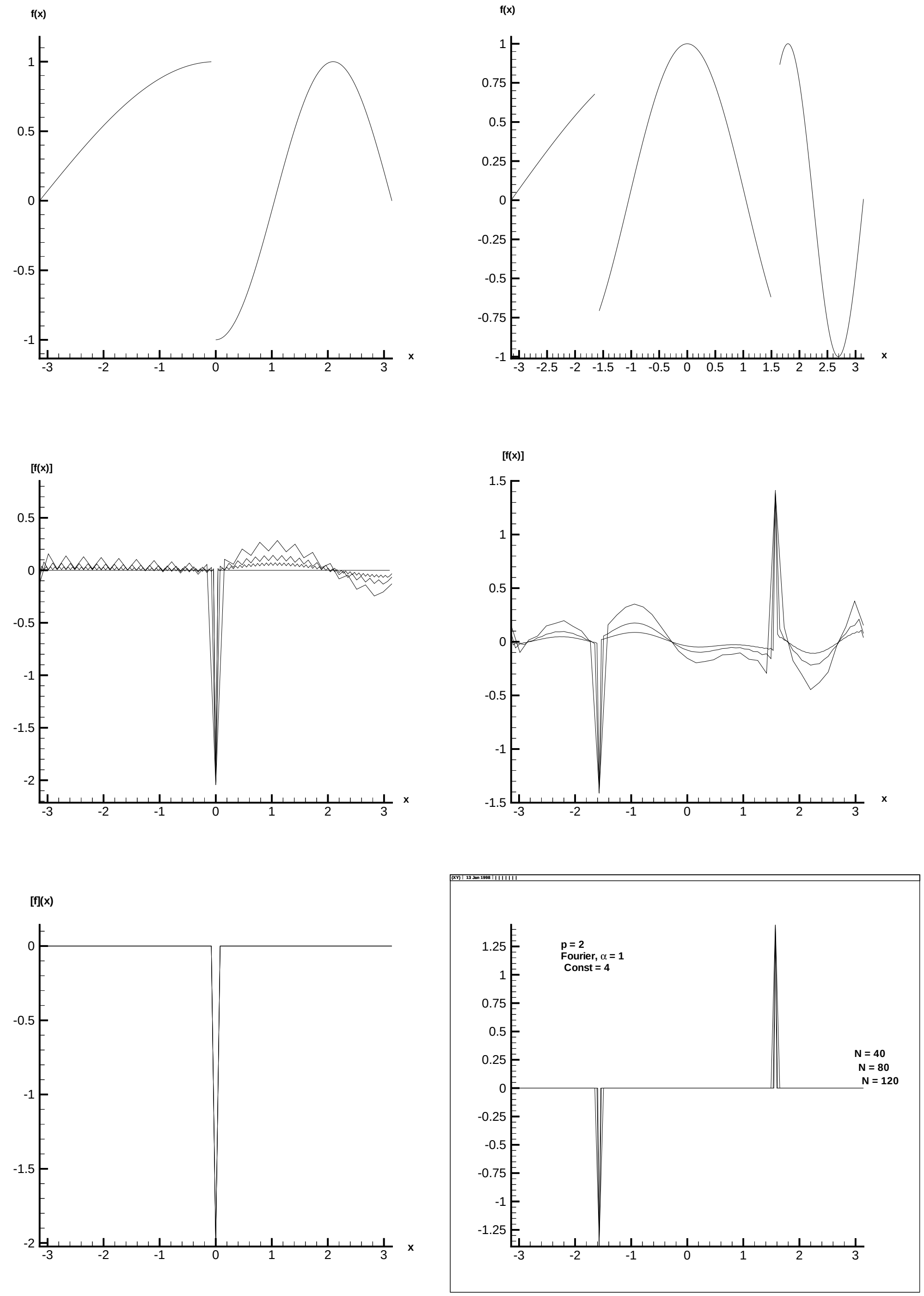

Detection of edges: concentration kernels, $S_N^\sigma[f]$, $N = 20, 40, 80$ with enhancement (*Gelb-Tadmor*)

Detection of edges – concentration kernels

(i) Odd kernels: $K_\varepsilon(-t) = -K_\varepsilon(t)$

(ii) Normalized: $-\int_{t\geq 0} K_\varepsilon(t)dt = 1 + \mathcal{O}(\varepsilon)$

(iii) Admissible: $|\int tK_\varepsilon(t)\varphi(t)dt| \leq Const.\varepsilon\|\varphi\|_{BV}$

Main result (Gelb-ET.): (i)— (iii) imply

$$K_\varepsilon(x) * f = [f](x) + \mathcal{O}(\varepsilon) \sim \begin{cases} \mathcal{O}(1), & x \sim singsupp[f] \\ \mathcal{O}(\varepsilon), & f(\cdot)_{|\sim x} \text{ smooth} \end{cases}$$

- Detection of edges by separation of scales:

⊙ concentration near edges of piecewise smooth f

- Local concentration kernels: $K_\varepsilon := \frac{1}{\varepsilon^2}\phi'(\frac{t}{\varepsilon}),\ \phi \in C_0^1(-1,1),\ \phi(0) = 1$

is admissible – concentrates near the origin $\int |tK_\varepsilon(t)|dt \leq Const \cdot \varepsilon$

⊙ Examples: Haar and bi-orthogonal moments

- Global kernels: $K_\varepsilon(t) \longleftrightarrow K_N(t)$

$$K_N^\sigma(t) := -\sum_{|k|\le N} \sigma(\frac{|k|}{N}) \sin kt, \qquad \sigma(\theta) \in C^2(0,1)$$

⊙ Computation: $K_N^\sigma * f \equiv K_N^\sigma * S_N[f]$

$$S_N^\sigma[f] := K_N^\sigma(x) * S_N[f] = i\pi \sum_{k=-N}^{N} sgn(k)\sigma(\frac{|k|}{N})\widehat{f}_k e^{ikx}$$

- Normalization: $-\int_{t\ge 0}^{\pi} K_N(t)dt = 2\sum_{0<k \text{ odd}} \frac{\sigma(\frac{k}{N})}{k} \sim \int_0^1 \frac{\sigma(\theta)}{\theta} \longrightarrow 1$

- Admissibility: 'heroic' cancelation of oscillations

$$K_N(t) = \sigma(1)\frac{\cos(N+\frac{1}{2})t}{2\pi \sin(t/2)} + Const.\left[\sigma(\frac{1}{N}) + \frac{1}{N}\sigma(1)\right] \times \frac{1}{t}$$

- Convergence rate: $|S_N^\sigma[f](x) - [f](x)| \le Const\left(\frac{\log N}{N} + |\sigma(\frac{1}{N})|\right)$

- Examples: concentration factors, $\sigma(\theta)$, $\theta = \frac{|k|}{N}$

⊙ 'Fourier' (*Banerjee & Geer*) $\boxed{\sigma^{\alpha}(\theta) \sim \sin(\alpha\theta)}$

⊙ 'Polynomial': $\boxed{\sigma^{p}(\theta) = p\theta^{p}}$

∘ $p = 1$ — (*Fejer*):

$$S_N^{p=1}[f](x) = i\pi \sum sgn(k) \frac{|k|}{N} \widehat{f}_k e^{ikx} = \frac{\pi}{N} S'_N[f](x)$$

∘ $p = 2$ — (global): $S_N^{p=2}[f](x) = \frac{\pi}{N^2}(H * S''_N[f])(x)$

⊙ 'Exponential'(*Gelb-ET.*) $\boxed{\sigma^{exp}(\theta) = Const.\theta \cdot e^{\frac{c}{\theta(\theta-1)}}}$

optimal localization:

$$S_N^{\sigma}[f](x) \sim \begin{cases} [f](x) \sim \mathcal{O}(1) & x \sim singsupp[f] \\ e^{-Const\sqrt{Nd(x)}} << 1 & otherwise \end{cases}$$

- Beyond periodicity: boundaries as edges...

Detection of edges in ψdospectral data

- Discrete data at: $x_\nu = -\pi + \nu\Delta x, \quad \Delta x := \frac{2\pi}{2N+1}$

$$T_N^\sigma[f](x) = \pi i \sum_{k=-N}^{N} sgn(k)\sigma(\frac{|k|}{N})\tilde{f}_k e^{ikx}, \quad \tilde{f}_k = \Delta x \sum f(x_\nu)e^{-ikx_\nu}$$

- Normalization: $\displaystyle\int_0^1 \frac{\pi\sigma(\theta)}{2\sin(\frac{\pi\theta}{2})}d\theta = 1$

- Main result (*Gelb-ET.*): detection of cells...

$$T_N^\sigma[f](x) \longrightarrow [f](x_{j+\frac{1}{2}}), \quad \xi \in [x_j, x_{j+1}]$$

⊙ Local differencing: $\Delta f_\nu := f(x_{\nu+1}) - f(x_\nu) = \left\{ \begin{array}{l} \mathcal{O}(1) \\ \mathcal{O}(\Delta x) \end{array} \right.$

⊙ Third-order: $\Delta^3 f_\nu = \left\{ \begin{array}{l} \mathcal{O}(1) \\ \mathcal{O}(\Delta x)^3 \end{array} \right\} \longleftrightarrow \sigma(\theta) \sim \sin^3(\frac{\pi\theta}{2})$

⊙ Exponential: $T_N^{exp}[f] = \left\{ \begin{array}{l} \mathcal{O}(1) \\ \mathcal{O}(e^{-\sqrt{d(x)/\Delta x}}) \end{array} \right.$

exponentially accurate; global; no real space realization

Enhancement

- Enhance Separation of Scales

$$(S_N^\sigma[f](x))^p \sim \begin{cases} N^{-p} & x \in \text{ smooth regions} \\ [f]^p(\xi) & \text{at jumps} \xi' s \end{cases}$$

$$N^{p/2}(S_N^\sigma[f](x))^p \sim \begin{cases} N^{-p/2} & x \in \text{ smooth regions} \\ N^{p/2}[f]^p(\xi) & \text{at jumps} \end{cases}$$

- Threshold for identifying an edge ——————————————>>> J_{crit}

$$S_N^{enhance}[f](x) = \begin{cases} S_N^\sigma[f](x) & \text{if } N^{p/2}|(S_N^\sigma[f](x))^p| > J_{crit} \\ 0 & \text{otherwise} \end{cases}$$

⊙ Examples

⊙ $K_\varepsilon(t) = \phi'_\varepsilon(t), p = 2$: Quadratic filter (*Svarek,..*) $(K_\varepsilon * f(x))^2 \longrightarrow [f]^2(x)$

⊙ Choose: N, $p \leq 5$, J_{crit} – small scale, $\sigma(\cdot)$ – exponential

- Nonlinear scale-free detection:

$$mimmod\{S_N^{p=1}, S_N^{exp}\} = \begin{cases} \min |S_N^{p=1}(x)|, |S_N^{exp}(x)| \\ 0 \qquad otherwise \end{cases}$$

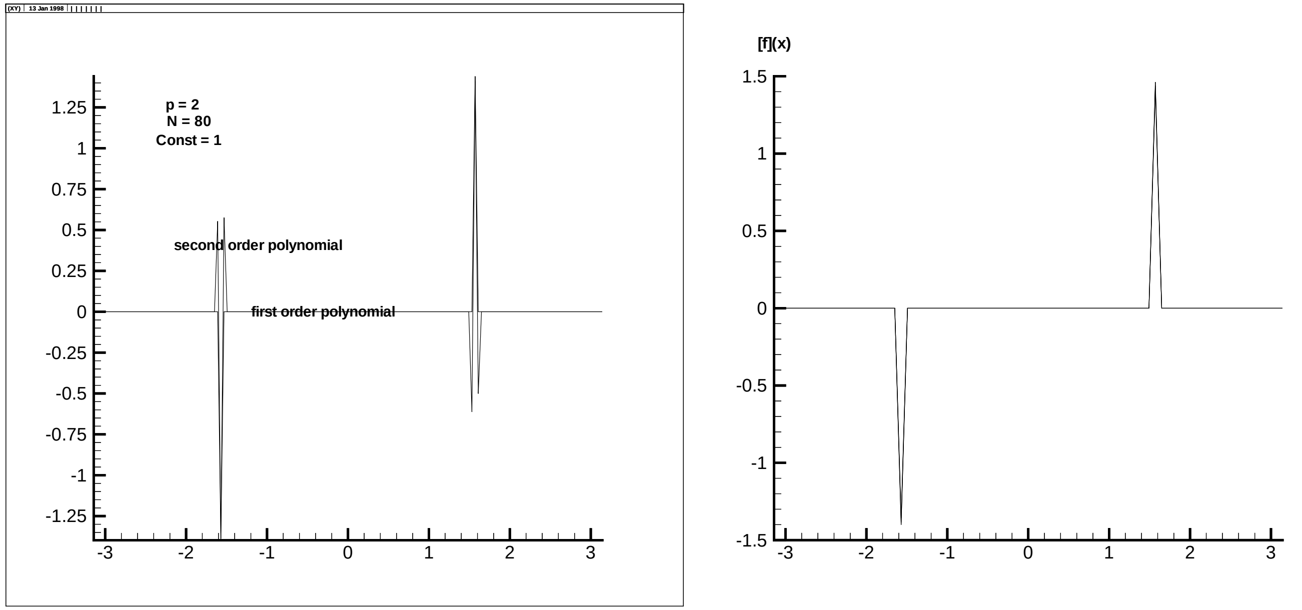

Enhanced detection of discontinuous edges using the conjugate sum, $S_N^\sigma[f](x) = i\pi \sum \sigma(\frac{|k|}{N}) sgn(k) \widehat{f}_k e^{ikx}$

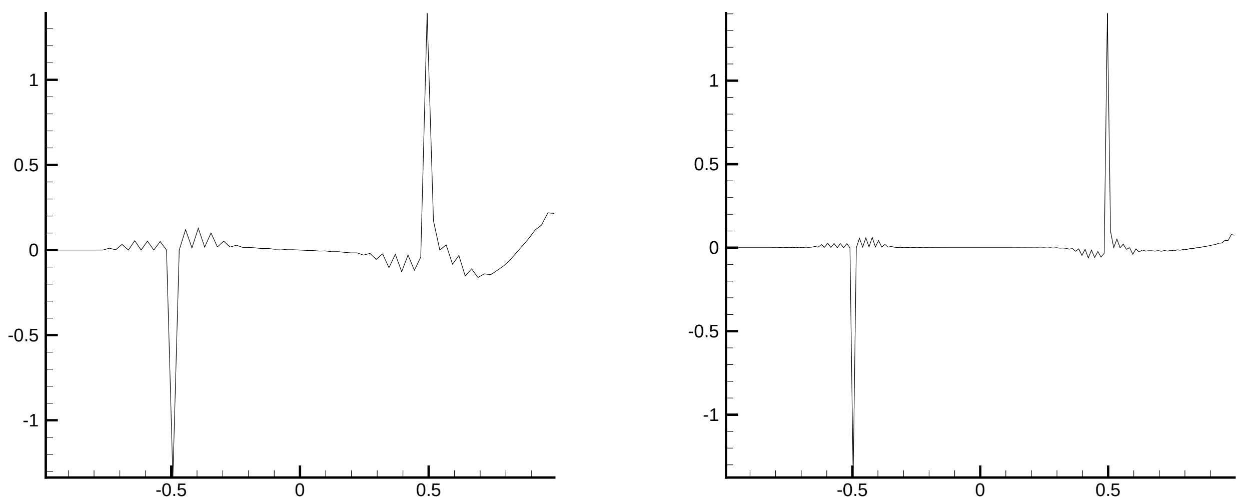

Detection by minmod cutoff $mm\{K^\xi, K^{exp}\}$, for $f_b(x)$ with jumps $[f](\pm\pi/2) = \pm\sqrt{2}$ (**left**) with $N = 40$ gridpoints and (**right**) with

$N = 80$ gridpoints (*Gelb-Tadmor*).

Enhanced Spectral Viscosity (SV) method

- Burgers' equation $u_t + \frac{1}{2}(u^2(x,t))_x = 0$

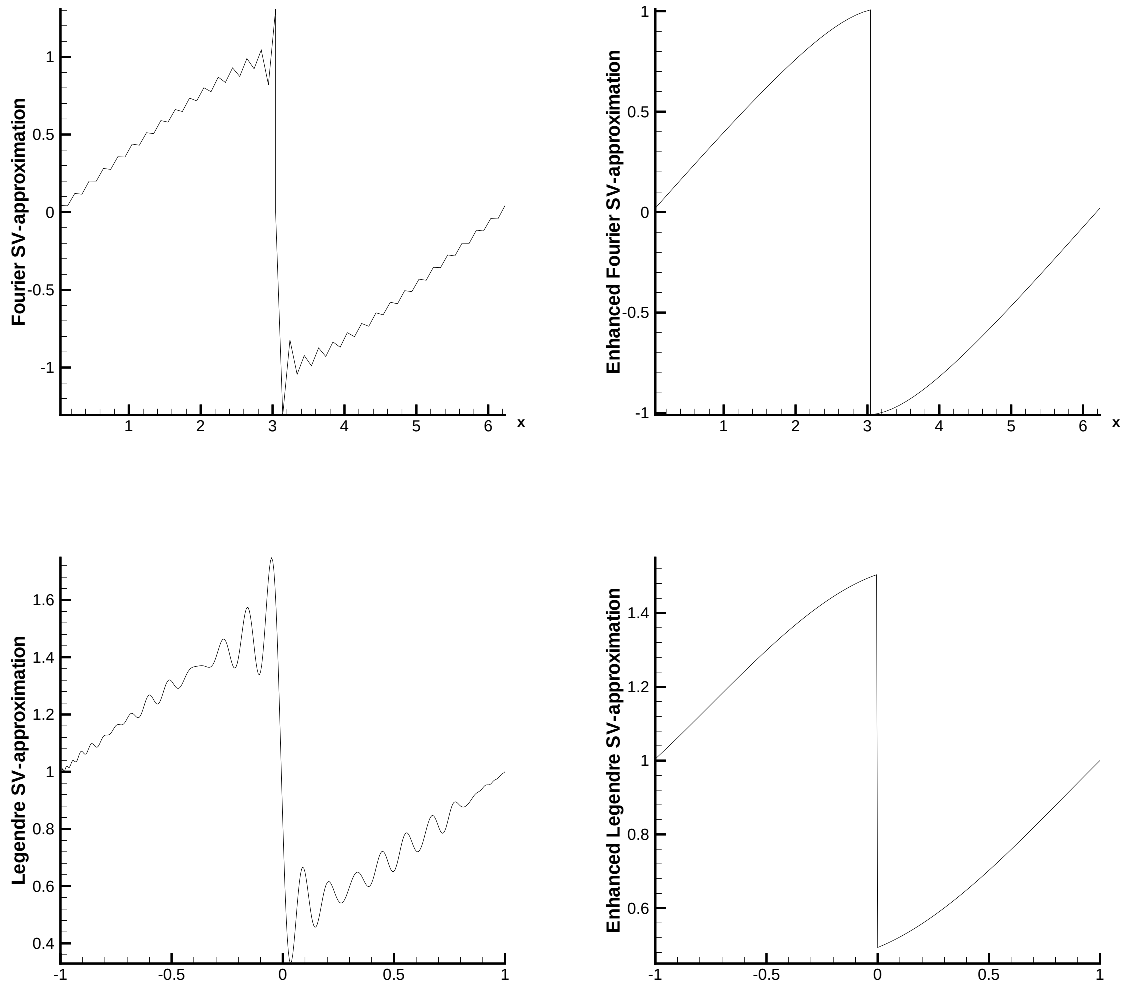

The solution of inviscid Burgers' eq., periodic boundary conditions using (left) the Legendre SV-approximation and (right) the enhanced SV-approximation for $N = 64$ modes (**Top**) Fourier and (**Bottom**) Legendre.

Shock tube problem– enhanced Legendre SV-method

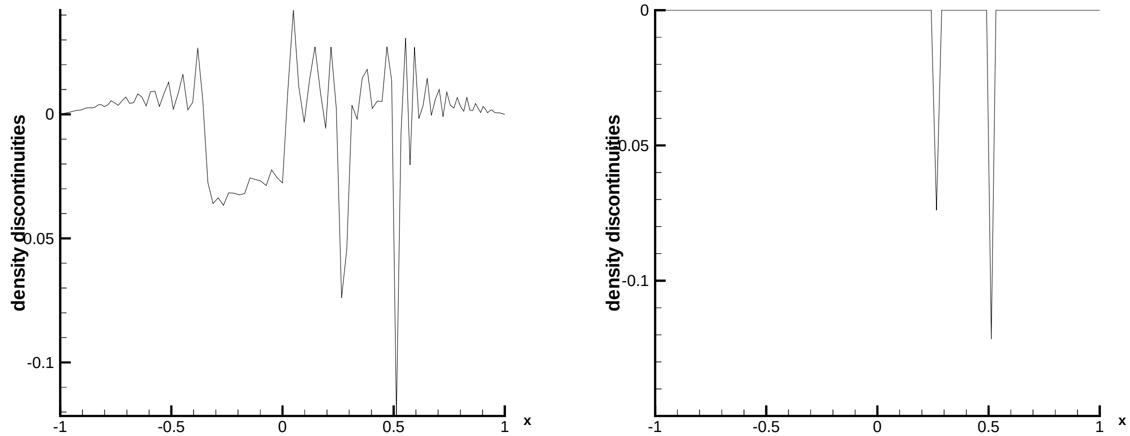

Detection of the shock discontinuities: (left) concentration kernel (right) with enhancement. $N = 128$ modes.

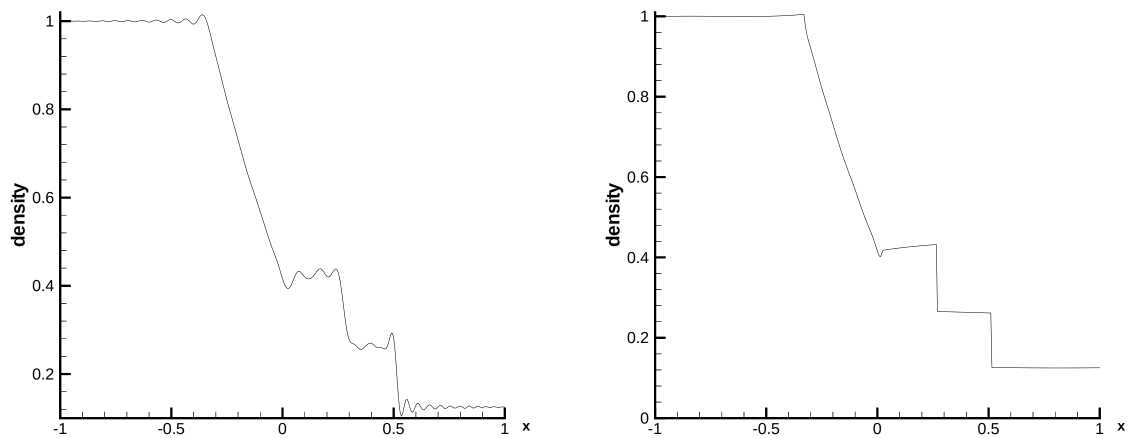

Density profile: (left) the Legendre SV-method and (right) after enhancement.

Detection of ‘kinks’

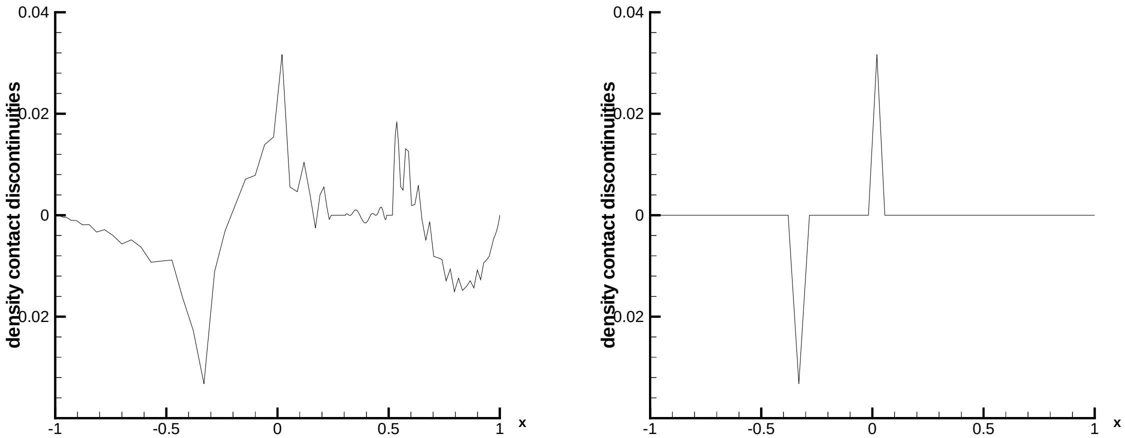

Detection of the contact discontinuities: (left) concentration kernel (right) with enhancement.

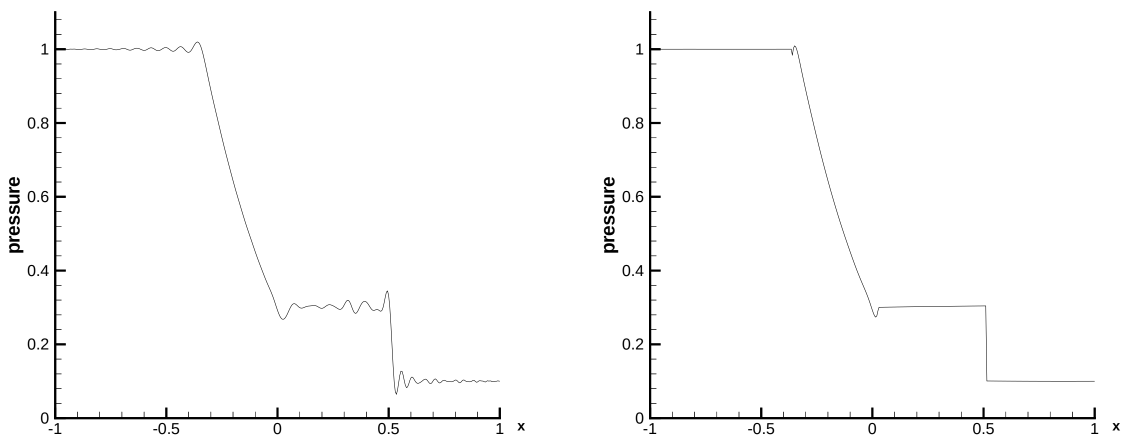

Pressure profile: (left) the Legendre SV-method and (right) the enhanced version.

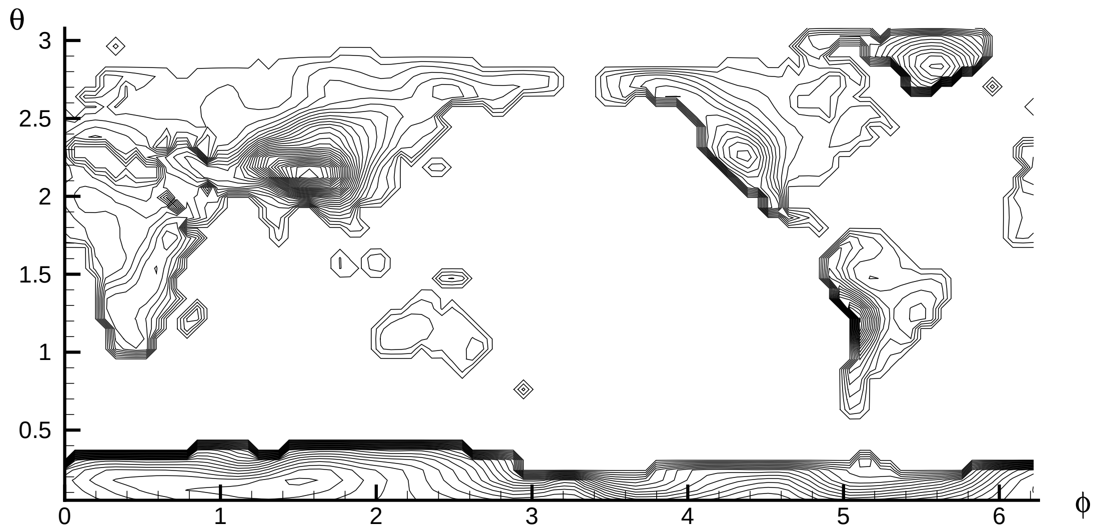
θ
3
2.5
2
1.5
1
0.5
0
1
2
3
4
5
6
ϕ

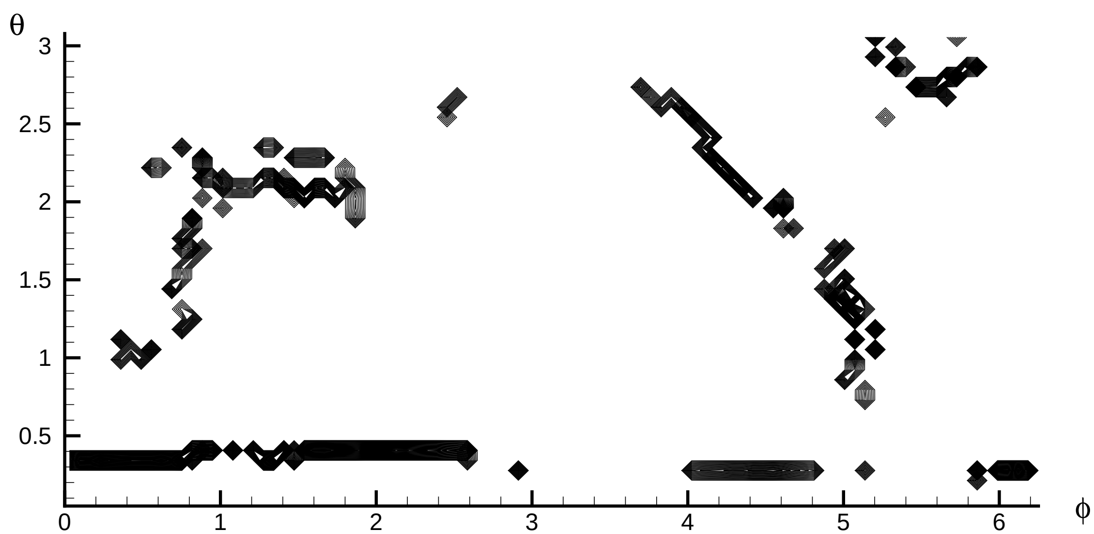
θ
3
2.5
2
1.5
1
0.5
0
1
2
3
4
5
6
ϕ

Spectral mollifiers

- One-parameter finite mollifiers:

$$\psi_\delta(x) =: \frac{1}{\delta}\psi(\frac{x}{\delta}), \quad \psi_\delta * f - f = \mathcal{O}(\delta^{p+1}) \downarrow 0$$

- Two-parameter spectral mollifiers (*Gottlieb-ET. 1985*)

⊙ Starting with...

$$\boxed{\psi(x) = \psi_p(x) := \rho(x) D_p(x)}$$

  - D_p — Dirichlet kernel of degree p, $D_p = \frac{\sin(p+\frac{1}{2})x}{2\pi \sin(x/2)}$
  - $\rho(x)$ — localized $\in C_0^\infty(-\pi,\pi)$ with $\rho(0) = 1$

⊙ ψ_p — highly oscillatory 'essentially' bump function as $p_N \uparrow \infty$

$$\int x^j \psi_p(x)dx = \begin{cases} 1 & j = 0 \\ 0 & j > 0 \end{cases} + \mathcal{O}(e^{-\sqrt{p}})$$

- We set

$$\boxed{\psi_{p,\delta} := \frac{1}{\delta}\psi_p(\frac{x}{\delta}) = \frac{1}{\delta}\rho(\frac{x}{\delta})D_p(\frac{x}{\delta})}$$

◦ Advantage of realizing data in physical space vs. . . . filtering: $\sum \widehat{\psi}(\frac{|k|}{N})\widehat{f}_k e^{ikx}$

Adaptive mollifiers — direction of smoothness

$\odot$ Set δ so $f(x-\delta y)\psi_p(y)$ admits largest domain of smoothness:

$\longleftrightarrow$ adaptive distance:

$$\boxed{\delta \sim d(x) := \text{dist}(x, \text{singsupp} f)}$$

- How to find $d(x)$? – detection of edges

- Where does the exponential accuracy come from?

'heroic' cancelation as $p = p(N) \uparrow$ with N

$\odot$ How to choose $p(N)$ — # of vanishing moments ...

$$p = p(N) \sim \begin{cases} \text{theoretical bound} :\sim \sqrt{N} & \textit{Gottlieb-ET. '85} \\ \text{computations} : \delta(x)N & \textit{ET.-Tanner '01} \end{cases}$$

Exponential Accuracy – Revisited $\psi_{p,\delta} = \frac{1}{\delta}\rho(\frac{x}{\delta})D_p(\frac{x}{\delta})$ (*ET.-Tanner*)

- Adaptive choice: $\delta(x) \sim d(x)$ and $p \sim \delta(x)N \sim d(x)N$

⊙ Higher order ('heroic') cancelation:

$$\int x^j \psi_{p,\delta}(x)dx \sim \left\{ \begin{array}{ll} 1 & j=0 \\ 0 & j>0 \end{array} \right\} + \mathcal{O}(e^{-Const.\sqrt{d(x)N}})$$

Ex $\rho(x) = e^{\frac{\alpha x^2}{x^2-\pi^2}} \in$ Gevrey regularity: $\|\rho\|_{C^s} \sim (s!)^2\eta^{-s}$

- Exponential accuracy

$$\left|\psi_{p,\delta} \star S_N f(x) - f(x)\right| \le C_\alpha \cdot d(x)N \cdot e^{-Const.\sqrt{d(x)N}}$$

- The discrete case — high-order 'expolants'

$$\left|\frac{\pi}{N}\sum_{\nu=0}^{2N-1}\psi_{p,\delta}(x-y_\nu)f(y_\nu) - f(x)\right| \le Const \cdot (d(x)N)^2 e^{-C\sqrt{d(x)N}}$$

⊙ Global exponential accuracy... except near edges where $\delta(x)N \sim 1$:

⊙ normalization ...

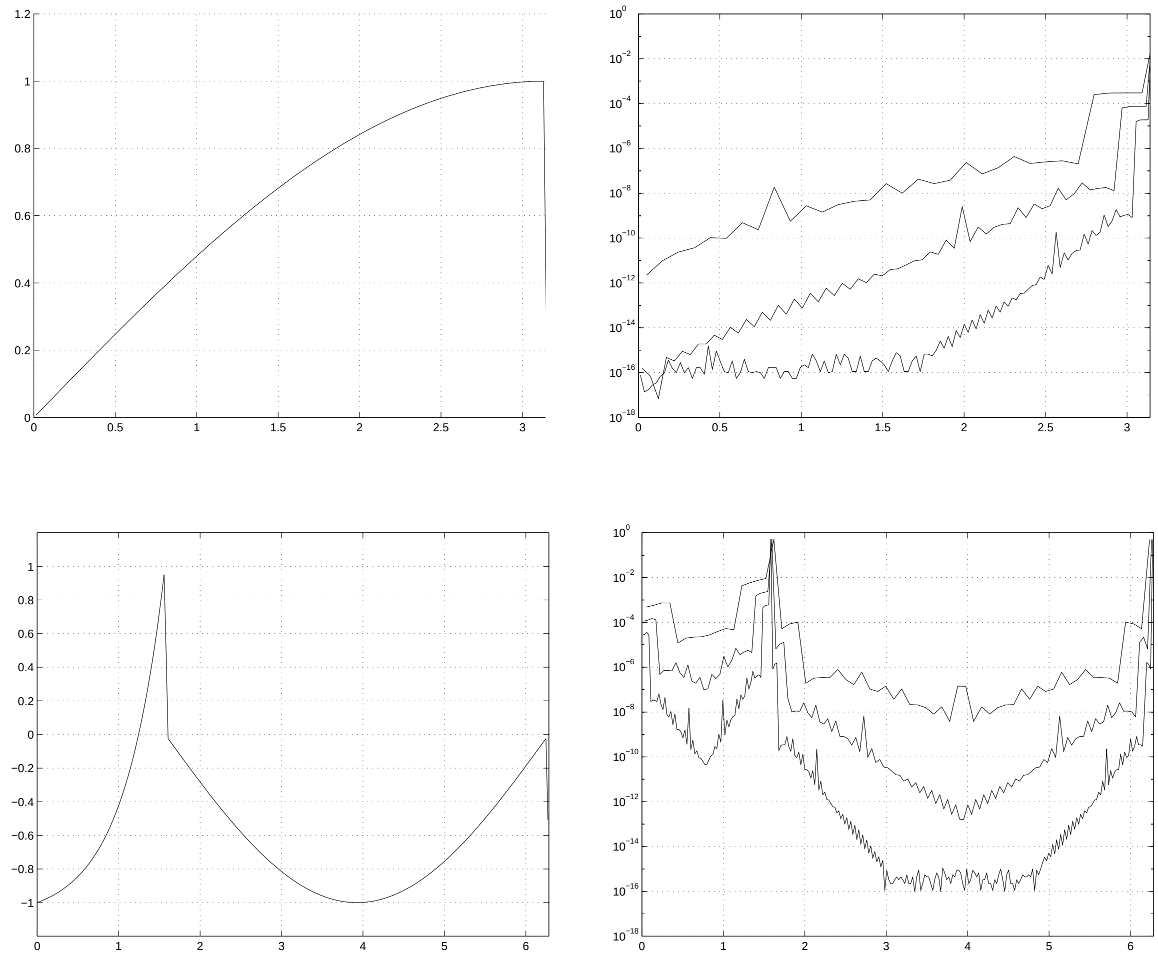

(**Left**): Recovery of $f(x)$ from its $N = 128$-modes spectral projections; Normalized mollifier, $\psi_{p,\theta}$ of degree $p = d(x)N/\pi\sqrt{e}$ (**Right**): Log error for recovery of $f(x)$ based on $N = 32, 64, 128$ modes (*Tadmor-Tanner*).

Looking forward...

- (piecewise-)Regularity spaces —

  interplay between theory and computations

- (genuinely-) multi-dimensional processing:

  ⊙ multidimensional detection

  ⊙ multidimensional reconstructions

... manipulate piecewise smooth data from its Radon transform

... decompose into normal and tangential directions

  - ... patterns, noise

- Interaction across range of scales

THE END